IOP Publishing New J. Phys. 25 (2023) 123024 https://doi.org/10.1088/1367-2630/ad0614

New Journal of Physics
The open access journal at the forefront of physics

Deutsche Physikalische Gesellschaft DPG
IOP Institute of Physics
Published in partnership with: Deutsche Physikalische Gesellschaft and the Institute of Physics

OPEN ACCESS

RECEIVED
7 June 2023

REVISED
19 September 2023

ACCEPTED FOR PUBLICATION
23 October 2023

PUBLISHED
11 December 2023

PAPER

Optimisation of the Tripathi model using a nuclear reaction cross-section database

F Luoni[1], C A Reidel[1], F Horst[1,2], U Weber[1] and M Durante[1,3,*]

1 Biophysics Department, GSI Helmholtzzentrum für Schwerionenforschung GmbH, Darmstadt, Germany
2 OncoRay—National Center for Radiation Research in Oncology, University Hospital Carl Gustav Carus, Technische Universität Dresden, Helmholtzzentrum Dresden-Rossendorf, Dresden, Germany
3 Technische Universität Darmstadt, Institut für Physik Kondensierter Materie, Darmstadt, Germany
* Author to whom any correspondence should be addressed.

E-mail: m.durante@gsi.de

Keywords: Tripathi model, hybrid-Kurotama model, nuclear reaction cross-sections, nuclear fragmentation, database, radiation protection in space, heavy-ion therapy

Abstract

Nuclear reaction cross-sections are an essential ingredient to reliable deterministic and stochastic radiation transport codes used for radiation protection in space and heavy-ion therapy applications. A recent study compared the existing literature data compiled within the open-access GSI-ESA-NASA cross-section database to the models implemented in the transport codes most commonly used for radiation protection in space and heavy-ion therapy applications. The outcome of the comparison was that none of the models fit well the experimental data for all projectile-target systems at all energy ranges. Therefore, the literature data were exploited to optimise the Tripathi–Cucinotta–Wilson model as reported in this work. This model is used as default in FLUKA, TRiP, and SpaceTRiP, it is part of the hybrid-Kurotama (HK) model used in particle and heavy ion transport code (PHITS), and it is implemented in Geant4. The consequences of using the proposed Tripathi–Cucinotta–Wilson optimisation in the HK model are also analysed.

1. Introduction

Realistic models for nuclear reaction cross-sections are an essential ingredient to reliable deterministic and stochastic radiation transport codes [1, 2], which are used for both the research fields of radiation protection in space [3, 4] and heavy-ion therapy [5, 6]. Therefore, a total reaction cross-section database was generated within a GSI-ESA-NASA collaboration [7] and made available open-access [8]. In [7], the collected data were compared to the semi-empirical models implemented in the Monte Carlo (MC) and deterministic codes most commonly used for radiation protection in space and heavy-ion therapy applications. The codes are Geant4 [9–12], particle and heavy ion transport code (PHITS) [13, 14], FLUKA [15, 16], HZETRN [17], TRiP [18], and SpaceTRiP [19]. The models are Tripathi–Cucinotta–Wilson (usually called 'Tripathi model' in the literature and in the MC codes), Kox, Shen, Kox–Shen, and hybrid-Kurotama (HK). The comparison shows that none of the models fit well the experimental data for all projectile-target systems of interest at all energy ranges.

Even though more accurate quark [20], optical [21, 22], and relativistic [23] models have been developed, the Tripathi model was chosen because it is used as default in FLUKA (with specific optimisations [16]), TRiP, and SpaceTRiP, it is part of the HK routine used in PHITS, and it is also implemented in Geant4. Additionally, it has many system-dependent free parameters that can be adjusted individually. The data collection was used to optimise the parameters of the Tripathi model so that it fits the existing literature data. A partial evaluation of the quality of the literature data was carried out within [7] and it was taken into account for the optimisation presented in this work. For example, data that were evaluated to under or overestimate the actual cross-section values were not included in the optimisation.

In this work, details of the proposed Tripathi model optimisations are provided, both for Tripathi96, which is used for systems where $A \leqslant 4$ for both the projectile and target nuclei) and Tripathi99, which is used for all other systems, i.e. light systems. The comparison of the optimised and the original model with literature data follows, for the case of some of the most important systems for space and heavy-ion therapy applications. Since the HK routine makes use of the Tripathi model, the consequences of the proposed Tripathi optimisations on the HK are systematically evaluated.

2. The Tripathi model

The Tripathi semi-empirical formula [24, 25] aims at modelling the total nuclear reaction cross-section as a function of the projectile kinetic energy. In particular, the so-called 'Tripathi99' parametrisation [25] is to be used for light systems, i.e. that at least either projectile or target has mass number $A \leqslant 4$, while the 'Tripathi96' parametrisation [24] for all other systems.

2.1. Tripathi96

The Tripathi96 model describes the total nuclear reaction cross-section as:

$$\sigma_\mathrm{R} = \pi {r_0}^2 \left({A_\mathrm{p}}^{1/3} + {A_\mathrm{T}}^{1/3} + \delta_E\right)^2 \left(1 - \frac{B}{E_\mathrm{cm}}\right) f, \tag{1}$$

where $r_0 = 1.1\,\mathrm{fm}$, A_p is the projectile mass number, A_T the target mass number, B is the energy-dependent Coulomb barrier, E_cm is the centre of mass kinetic energy, and f is a multiplication factor equal to 1 in all cases but for $^1\mathrm{H} + {}^4\mathrm{He}$ and $^1\mathrm{H} + {}^{12}\mathrm{C}$, where it is supposed to be set to 27 and 3.5, respectively. δ_E is defined as:

$$\delta_E = 1.85\,S + 0.16 \frac{S}{{E_\mathrm{cm}}^{1/3}} - C_E + \alpha \frac{(A_\mathrm{T} - 2Z_\mathrm{T})\,Z_\mathrm{p}}{A_\mathrm{T} A_\mathrm{p}}, \tag{2}$$

where $\alpha = 0.91$ and:

$$C_E = D\left(1 + \exp\left(-E/T_1\right)\right) - A\exp\left(-E/792\right)\cos\left(0.229 E^{0.453}\right). \tag{3}$$

$A = 0.292$, $T_1 = 40$, E is the projectile kinetic energy, and:

- for the proton–nucleus case: $D = 2.05$,
- for the case of ^{4}He projectiles:

$$D = D_0 - 8.0 \times 10^{-3} A_\mathrm{T} + 1.8 \times 10^{-5} {A_\mathrm{T}}^2 - \frac{0.8}{1 + \mathrm{e}^{\frac{250-E}{G}}}, \tag{4}$$

  where $D_0 = 2.77$ and $G = 75$,
- for all other cases:

$$D = d\,\frac{\rho_{A_\mathrm{p}} + \rho_{A_\mathrm{T}}}{\rho_{A_\mathrm{C}} + \rho_{A_\mathrm{C}}} \tag{5}$$

  where $d = 1.75$, with the exception of lithium nuclei, where the outcome of equation (5) is supposed to be divided by 3.

More details about the Tripathi96 model can be found in [24].

2.2. Tripathi99

The Tripathi99 formula [25] describes the the total nuclear reaction cross-section for light systems as:

$$\sigma_\mathrm{R} = \pi {r_0}^2 \left({A_\mathrm{p}}^{1/3} + {A_\mathrm{T}}^{1/3} + \delta_E\right)^2 \left(1 - R_\mathrm{c}\frac{B}{E_\mathrm{cm}}\right) X_m. \tag{6}$$

Details about the parameters can be found in [25]. Differently from Tripathi96, T_1 and G are system dependent. To be noted that in [25], an energy and target-dependent expression for the X_m parameter is given. Nevertheless, it is discussed in detail in [7] that using $X_m = 1$ for every projectile but neutrons gives better agreement with the data and with the plots presented in [25] itself. $X_m = 1$ is also used in the PHITS subroutine.

Table 1. Recommendations for parameters to be used for Li isotopes projectiles within Tripathi96. In [24], $T_1 = 40$, $d = 1.75$, and $f = 1$ for all of the systems.

System	T_1	d	f	System	T_1	d	f
^{6}Li → ^{9}Be	110	1.8	1.1	^{7}Li → ^{9}Be	40	1.65	1
^{12}C	110	1.75	1	^{27}Al	40	1.8	1
^{27}Al	110	1.9	1.05	^{28}Si	40	1.6	1
^{28}Si	110	1.8	0.95	^{56}Fe	40	2	1
^{64}Cu	100	1.8	1	^{64}Cu	100	1.8	1
^{8}Li → ^{9}Be	40	1.65	1	^{9}Li → ^{12}C	40	1.8	1
^{28}Si	80	1.8	0.93	^{27}Al	40	1.9	1
^{64}Cu	100	1.8	1	^{64}Cu	100	1.8	1
^{11}Li → ^{9}Be	40	1.3	1				
^{12}C	40	1.35	1				
^{28}Si	55	2.8	1.5				
^{64}Cu	100	1.8	1				

3. Optimisation of the Tripathi96 model

Thanks to the large amount of data collected in the reaction cross-section database [7], it was possible to optimise the Tripathi parametrisation so that it fits the pool of existing literature data better. A detailed description of the Tripathi96 and 99 models can be found in [7, 24, 25]. In particular, the specific parameter names correspond to the ones that can be found in [7]. For what concerns the Tripathi96 parametrisation, the following modifications are proposed.

3.1. Lithium projectiles

Tripathi *et al* [24] recommends the usage of $D/3$ instead of the D parameter for lithium projectiles for the Tripathi96 model calculations. However, the usage of D gives better agreement with the experimental data. Additional optimisations are also proposed. The parameters that were modified with respect to [24] are T_1, d, and f. The optimisation process was applied also to lithium isotopes other than ^{7}Li for completeness. Such optimisations are reported in table 1. To be noticed that the optimisations are not only valid for the case of lithium projectiles impinging on the specified targets, but also for the case of inverse kinematics. For example, optimisations are proposed for the system ^{6}Li → ^{9}Be, but they are also applied for ^{9}Be → ^{6}Li. These optimisations are proposed here and not e.g. for ^{9}Be projectiles because the Tripathi model implementations always use the lightest nucleus as the projectile.

The results of the fit of the optimised model with literature data are presented in figure 1. The focus was put on systems of interest for radiation protection in space. Lithium could play in fact, an important role as potential innovative shielding material against cosmic radiation [26–29] and ^{9}Be, ^{12}C, ^{28}Si, and ^{56}Fe are among the main contributors to the galactic cosmic radiation (GCR) spectrum [4, 30]. To be noticed that ^{7}Li + ^{12}C required no specific optimisations (see panel (b) of figure 1) but the usage of the D parameter instead of $D/3$. Examples of the optimisation of all lithium isotopes impinging on ^{9}Be targets can be found in figure 2.

3.2. Other projectiles

Optimisations for several other systems are reported in table 2. Additionally to the parameters found in [7], b appears. b is the multiplication factor of the B energy-dependent Coulomb-barrier parameter of [24]. In [24], it is always set to 1.44. Also in this case, the optimisations are valid in inverse kinematics as well. Therefore, heavy ions do not appear as projectiles but only as targets since the lighter ions always play the role of projectiles in the Tripathi model implementations.

Figures 3–7 show the original and optimised Tripathi96 model together the literature experimental data for the main contributors to the GCR spectrum, i.e. ^{9}Be, ^{12}C, ^{16}O, ^{20}Ne, ^{24}Mg, ^{28}Si, and ^{56}Fe, as projectiles. In addition, ^{12}C ions are used for radiation therapy [37, 38] and oxygen was also proposed to be used for therapy applications [39]. The chosen targets are: ^{12}C, ^{16}O, ^{24}Mg, ^{27}Al, ^{28}Si, and ^{40}Ca because of the relative importance of these isotopes in the human body, in the spacecraft structure and electronics, and in the composition of *in situ* potential shielding materials. O, Mg, Al, Si, and Ca are, in fact, main components of Moon and Mars regolith. In addition, also the ^{9}Be + ^{64}Cu system is shown in figure 3 because it required the larger parameter modifications (see table 2). If no experimental data have been measured for a combination of the above-mentioned projectile-target, the combination is not shown in figures 3–7. The only exceptions are the following systems:

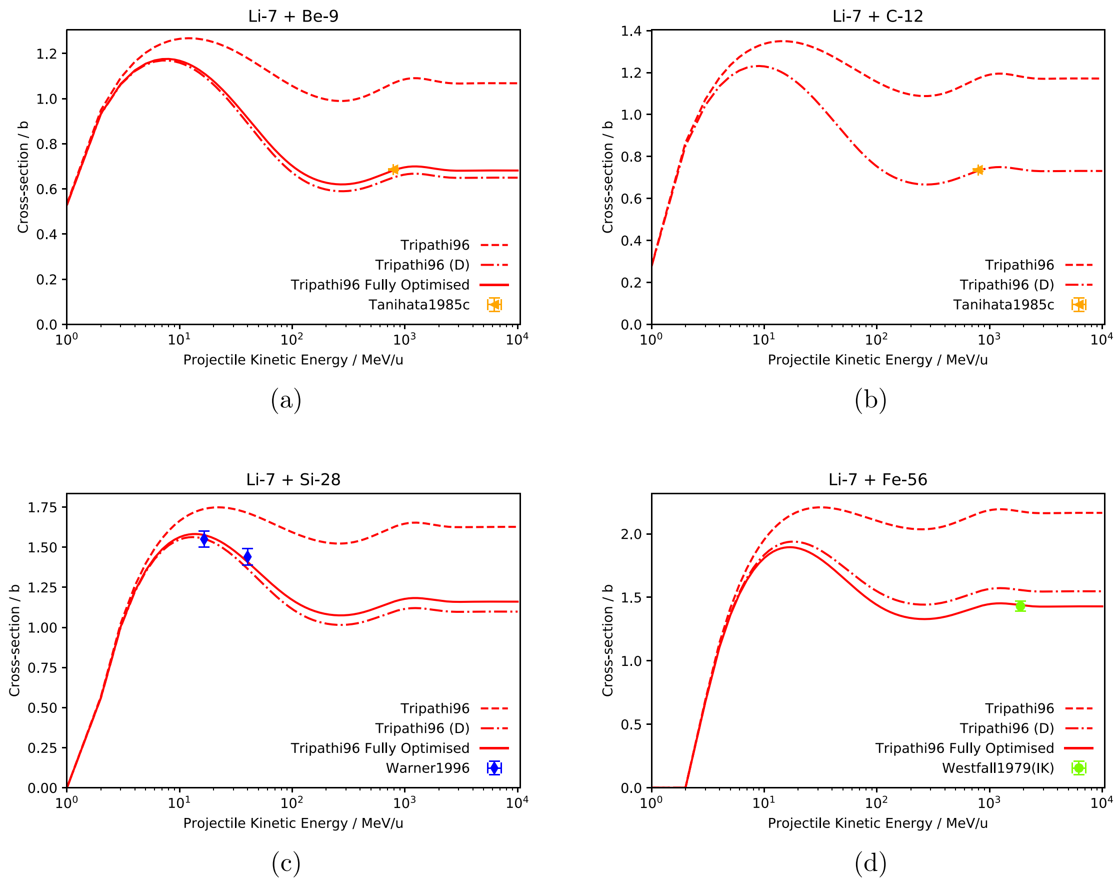

Figure 1. Tripathi96 computed both using the original Tripathi96 model [24], which recommends to make use of $D/3$, $T_1 = 40$, $d = 1.75$, and $f = 1$, the Tripathi model using D instead of $D/3$ without modifying any other parameter, and the fully optimised Tripathi model as recommended within the present work (see table 1). IK stands for inverse kinematics. Data in panels (a) and (b) are from [31], in panel (c) from [32] and in panel (d) from [33].

- ^{12}C + ^{24}Mg, because the original Tripathi96 model fits the data perfectly, and
- ^{16}O + ^{27}Al and ^{20}Ne + ^{27}Al, for which only literature data from the Kox1987 dataset [40] were measured. Since this dataset was evaluated to systematically underestimate actual cross-section values [7], optimisations were not done based on it.

Also ^{10}C, ^{11}C, ^{14}O, and ^{15}O were included in the optimisation because of the potential live imaging advantages in using them for radiation therapy [54–57]. Optimisations are reported in table 3 and figure 8. Only ^{12}C is shown as target because of its relative importance in the human body.

4. Optimisation of the Tripathi99 model

From a deep analysis of all light ($A \leqslant 4$) nucleus–nucleus systems in the data collection, new parameters are recommended to be used for ^{2}H, ^{3}He and ^{4}He projectiles. For all cases, it is recommended to use $\alpha = 5$ for the multiplication factor of the neutron excess parameter for $Z_T > 54$. Using $\alpha = 0.91$, in fact, underestimates cross-sections for very heavy targets.

4.1. ^{2}H projectiles

Deuterons are neither very important for radiation protection in space nor for radiation therapy, but are of interest for other technical applications, e.g. neutron production at accelerator facilities. Therefore, ^{2}H projectiles were also included in this study for completeness. Tripathi *et al* [25] suggests to use the following equation if the target is ^{4}He:

$$D = 1.65 + \frac{0.22}{1 + \exp\left(\left(500 - x\right)/200\right)}, \tag{7}$$

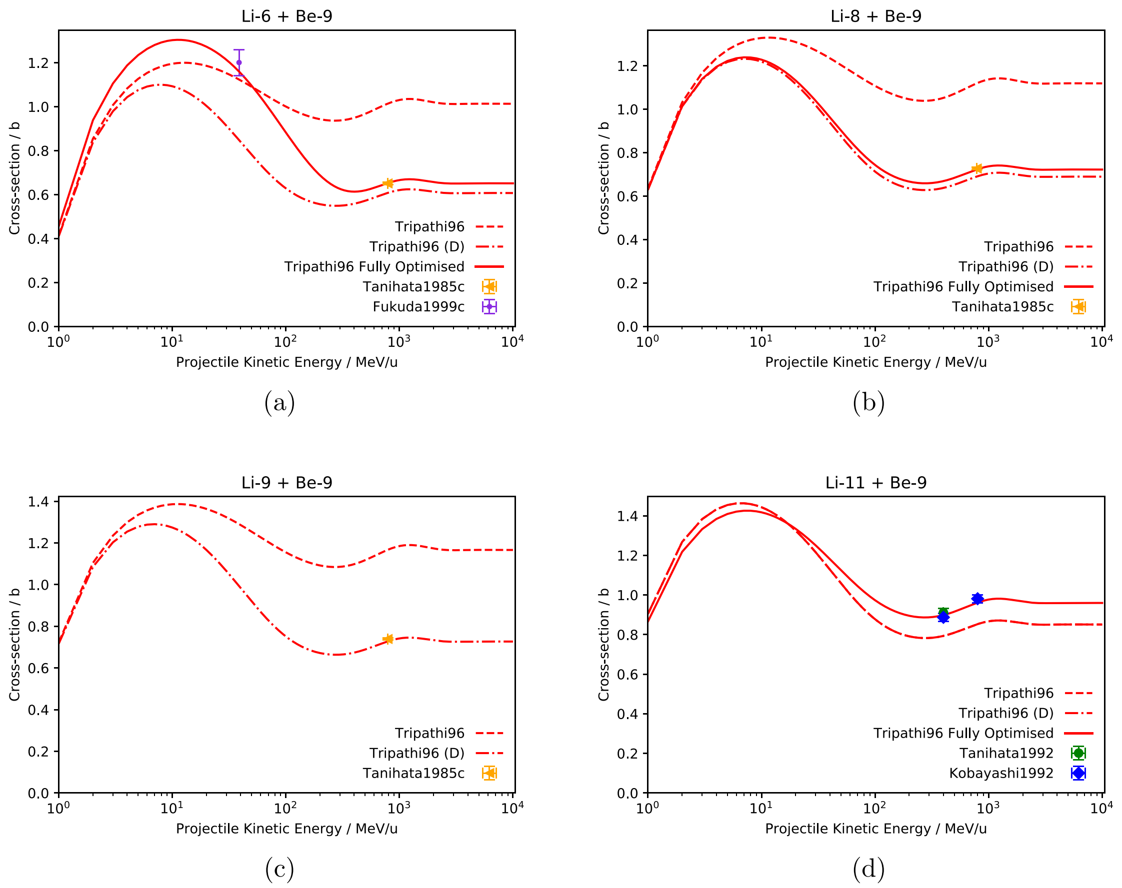

Figure 2. Tripathi96 computed both using the original Tripathi96 model [24], which recommends to make use of $D/3$, $T_1 = 40$, $d = 1.75$, and $f = 1$, the Tripathi model using D instead of $D/3$ without modifying any other parameter, and the fully optimised Tripathi model as recommended within the present work (see table 1). Data in panel (a) are from [31, 34], in panels (b) and (c) from [31], in panel (d) from [35, 36].

Table 2. Recommendations for parameters to be used for different projectiles within Tripathi96. In [24], $T_1 = 40$, $d = 1.75$, $A = 0.292$, $f = 1$, and $b = 1.44$ for all of the systems.

System	T_1	d	A	f	b	System	T_1	d	A	f	b
$^{12}C \rightarrow {}^{12}C$	50	1.9	0.292	1	1.44	$^{9}Be \rightarrow {}^{9}Be$	40	1.7	0.292	1	1.44
^{16}O	40	2	0.292	1	1.44	^{12}C	65	1.8	0.292	1	1.44
^{20}Ne	30	2.7	0.292	1.4	1.44	^{27}Al	40	1.8	0.292	1	1.44
^{22}Na	80	2.1	0.292	1	1.44	^{56}Fe	40	1.8	0.292	1	1.44
^{24}Mg	55	1.9	0.292	1	1.44	^{64}Cu	40	4	0.292	2.2	6
^{27}Al	50	2	0.292	1	1.44	$^{16}O \rightarrow {}^{64}Cu$	30	1.75	0.292	1	1.44
^{28}Si	70	1.9	0.292	1	1.44	$^{20}Ne \rightarrow {}^{64}Cu$	60	1.75	0.292	1	1.44
^{40}Ca	50	2.2	0.292	1	1.44						
^{56}Fe	55	2.2	0.292	1	1.44						
^{64}Cu	60	1.9	0.292	1	1.44						

and for all other targets:

$$D = 1.65 + \frac{0.1}{1 + \exp\left(\left(500 - x\right)/200\right)}. \tag{8}$$

In this work, it is recommended to use

$$D = 1.72 + \frac{0.1}{1 + \exp\left(\left(500 - x\right)/200\right)} \tag{9}$$

for the specific case of ^{2}H targets and

$$D = 1.65 + \frac{0.22}{1 + \exp\left(\left(500 - x\right)/100\right)} \tag{10}$$

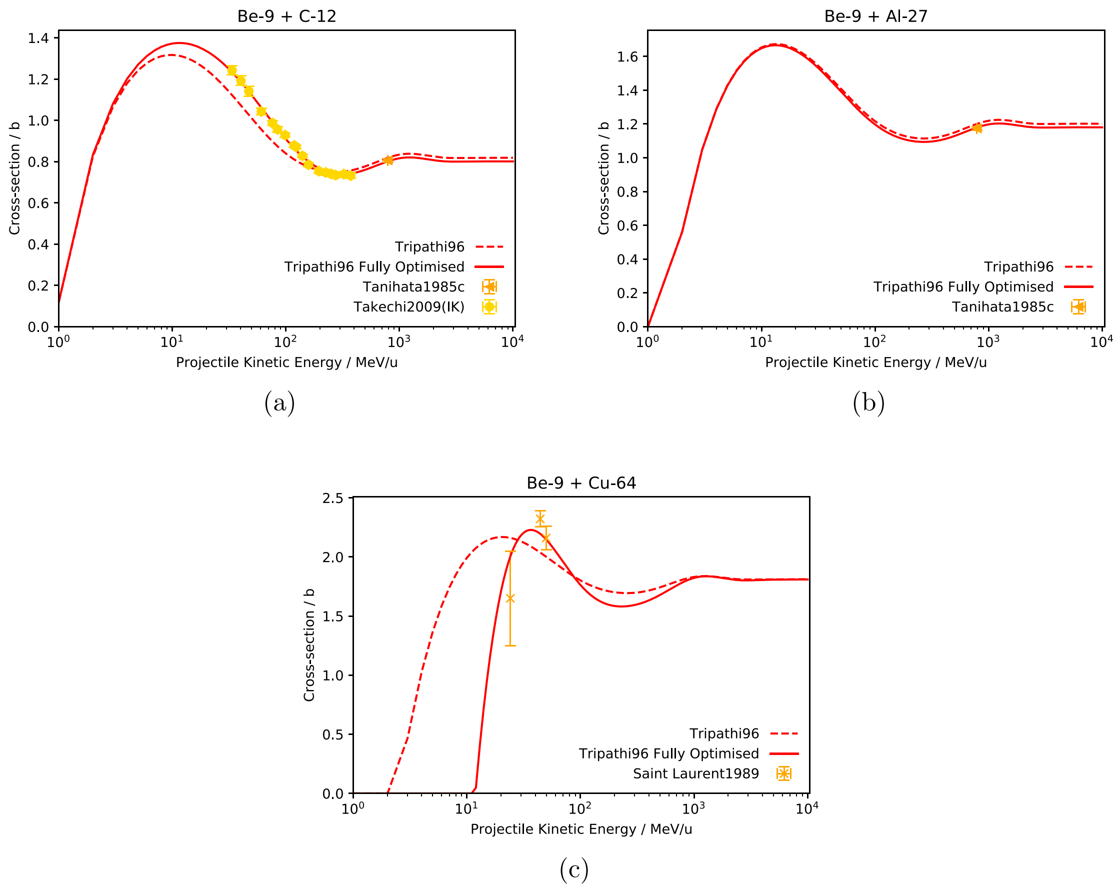

Figure 3. Tripathi96 computed using the original Tripathi96 model [24] and the fully optimised Tripathi model as recommended within the present work (see table 2). IK stands for inverse kinematics. Data in panel (a) are from [31, 41], in panel (b) from [31], and in panel (c) from [42].

for ^{4}He targets. The results of the application of equations (9) and (10) to the Tripathi99 model are shown in figure 9. For heavier targets, recommendations for the R_C, T_1, A, X_m, and D parameters are given in table 4 for every system for which literature data are available [7].

The optimisations proposed for ^{2}H on the targets of interest for space and therapy applications listed earlier in this work, are reported in figure 10. For ^{2}H + ^{12}C and ^{2}H + ^{27}Al, the agreement is shifted from the Wilkins1962 dataset to Mayo1965 because Mayo1965 data are an upgraded version of Wilkins1962. Same was done for other systems that are not reported in figure 10. For the cases in which only Wilkins1962 are available, no optimisations are proposed.

4.2. ^{3}He projectiles

For ^{3}He projectiles, additional recommendations for R_C and T_1 are given in table 5. Since no high-energy data are found in literature, no changes in D were proposed.

The optimisations of ^{3}He impinging on the targets of interest for space and therapy applications, are reported in figure 11. ^{3}He-ions have in fact, been recently discussed for heavy-ion therapy applications [64]. The systems for which no experimental data were measured or no optimisation was proposed are not reported in the figure.

4.3. ^{4}He projectiles

Concerning ^{4}He projectiles, they are very significant both concerning space [66] and heavy-ion therapy applications [67–69]. The following optimization of Tripathi96 D parameter has been proposed [70, 71] for the case of ^{4}He projectiles on targets with masses between C and Si:

$$D = D_0 - 8.0 \times 10^{-3} A_T + 1.8 \times 10^{-5} {A_T}^2 - \frac{0.3}{1 + e^{\frac{120-E}{G}}}, \tag{11}$$

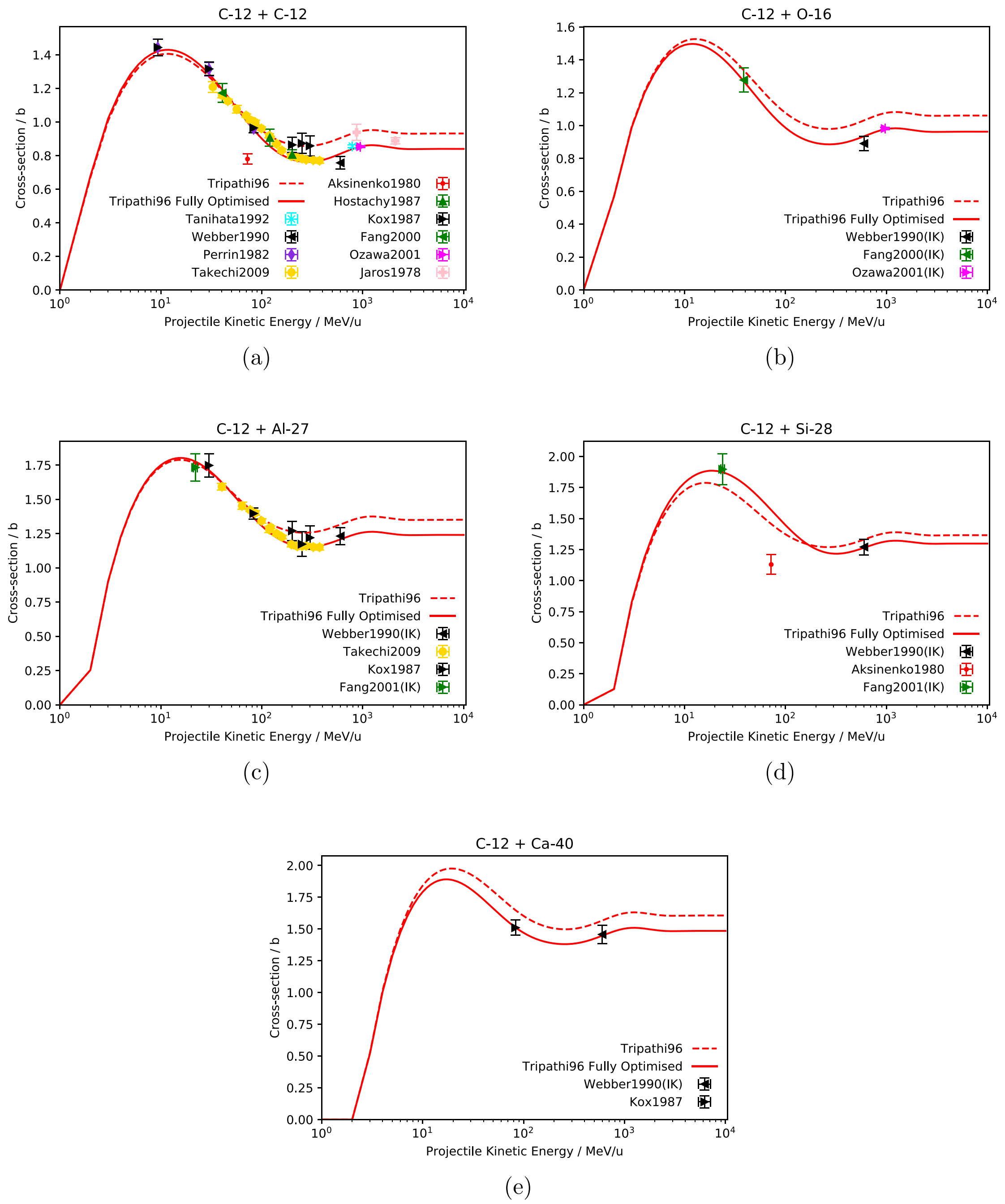

Figure 4. Tripathi96 computed using the original Tripathi96 model [24] and the fully optimised Tripathi model as recommended within the present work (see table 2). IK stands for inverse kinematics. Data in panel (a) are from [35, 40, 41, 43–49], in panel (b) from [43, 47, 48], in panel (c) from [40, 41, 43, 50], in panel (d) from [43, 45, 50], and in panel (e) from [40, 43].

where $D_0 = 2.2$ and $G = 50$. The optimisation was based on data from [71–73] and on the subsequent improvements of ^{4}He dose calculations [5, 70]. Nevertheless, Tripathi99 is the model that should be used for the case of ^{4}He projectiles. The proposed changes to the Tripathi99 model are reported table 6 and they involve parameters R_C, T_1, and A. Recommendations are also given about which equation to use in the Tripathi99 calculations between 4 and 11—even if equation (11) was originally proposed for ^{4}He projectiles within Tripathi96 [71]—and what associated G and D_0 values. Among the other things, it can be noticed that an increase in D_0 with A_T gives a systematic better fit with the high-energy data.

The optimisations proposed for ^{4}He on the targets of interest for space and therapy applications, are reported in figure 12.

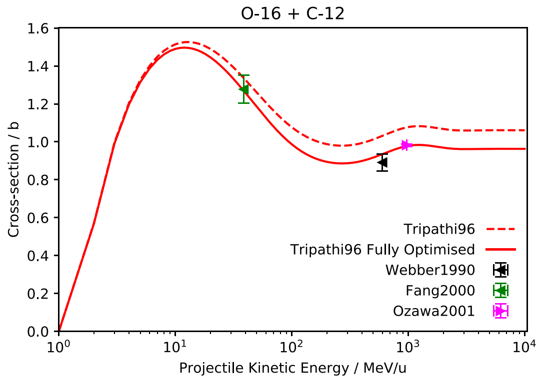

(a)

Figure 5. Tripathi96 computed using the original Tripathi96 model [24] and the fully optimised Tripathi model as recommended within the present work (see table 2). Data are from [43, 47, 48]. The optimised parameters can be found in table 2 for $^{12}C + ^{16}O$, since the lightest ion is always used by the model as projectile.

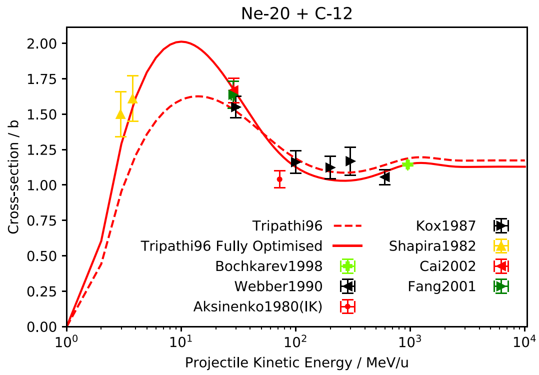

(a)

Figure 6. Tripathi96 computed using the original Tripathi96 model [24] and the fully optimised Tripathi model as recommended within the present work (see table 2). IK stands for inverse kinematics. Data are from [40, 43, 45, 50–53].

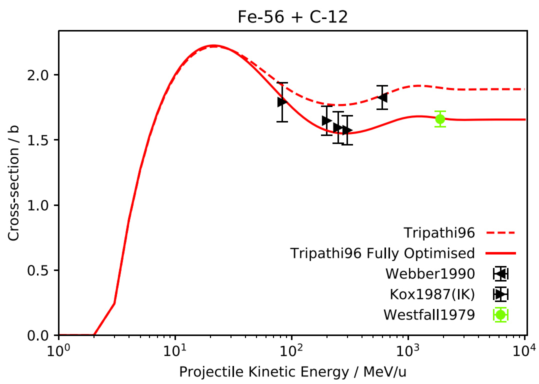

(a)

Figure 7. Tripathi96 computed using the original Tripathi96 model [24] and the fully optimised Tripathi model as recommended within the present work (see table 2). IK stands for inverse kinematics. Data are from [33, 40, 43].

Table 3. Recommendations for values of the d parameter to be used within Tripathi96 for the radioactive ions ^{10}C, ^{11}C, ^{14}O, and ^{15}O. In [24], $d = 1.75$ for all systems. The other parameters ($T_1 = 40$, $A = 0.292$, and $f = 1$) remain unchanged.

System	d
$^{10}\mathrm{C} \rightarrow {}^{12}\mathrm{C}$	1.9
$^{11}\mathrm{C} \rightarrow {}^{12}\mathrm{C}$	2.1
$^{14}\mathrm{O} \rightarrow {}^{12}\mathrm{C}$	1.95
$^{15}\mathrm{O} \rightarrow {}^{12}\mathrm{C}$	1.95

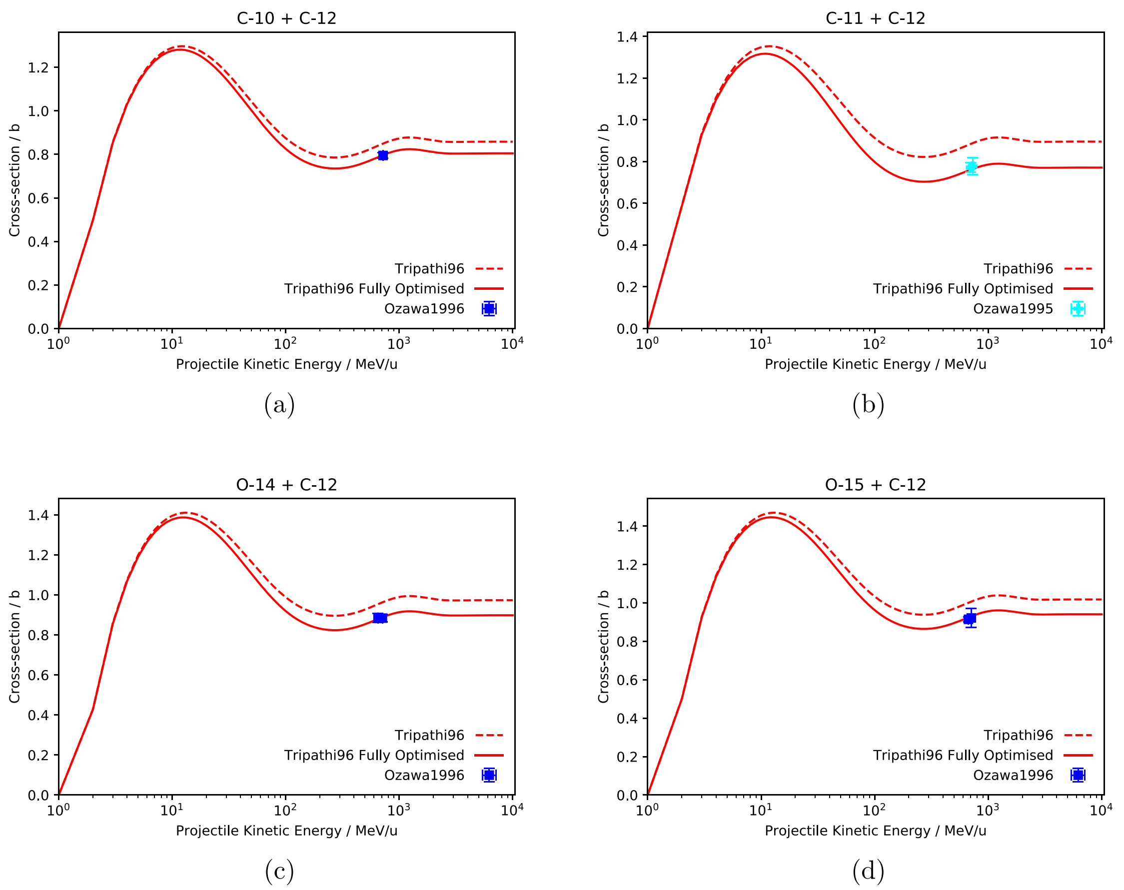

Figure 8. Tripathi96 computed using the original Tripathi96 model [24] and the fully optimised Tripathi model as recommended within the present work (see table 3). Data in panels (a), (c), and (d) are from [58], in panel (b) from [59].

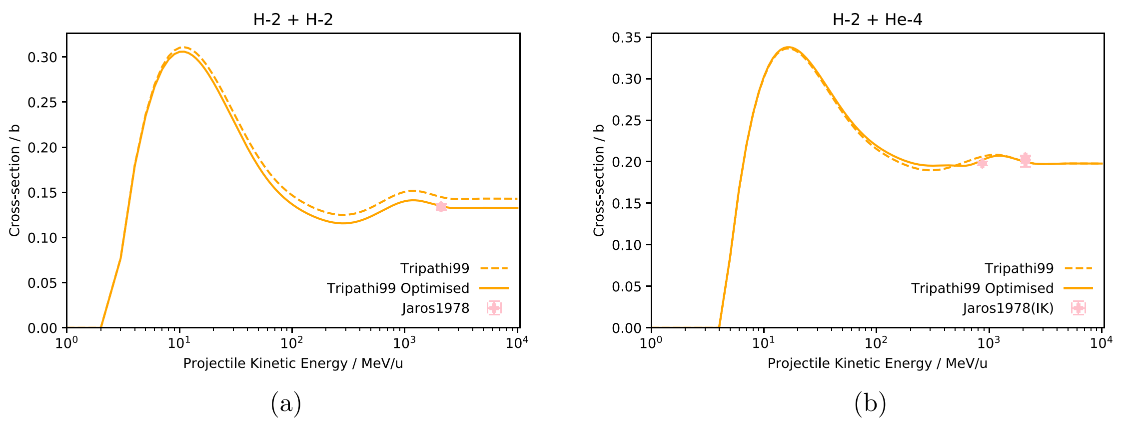

Figure 9. Comparison between the results obtained for $^2\mathrm{H} + {}^2\mathrm{H}$ and $^2\mathrm{H} + {}^4\mathrm{He}$ using, respectively, equations (7) and (8) versus equations (9) and (10) in the Tripathi99 model. The experimental data from the database are plotted as well. IK stands for inverse kinematics. Data are from [49].

Table 4. Recommendations for parameters R_C, T_1, A, X_m, and α to be used for ^{2}H projectiles in Tripathi99 [25]. The parameters from the original model as implemented in PHITS are compared to the parameters recommended in this work. In particular, in the PHITS implementation, the parameters presented within [25] plus specific ones for $^2\mathrm{H}+{}^4\mathrm{He}$ are used. In addition, $X_m = 1$ is used. Systems that did not require any change in these parameters with respect to the PHITS implementation (e.g. $^2\mathrm{H}+{}^2\mathrm{H}$, ^{4}He) are not reported.

	Tripathi99 [25] as implemented in PHITS [7]						This work					
System	R_C	T_1	A	X_m	D	α	R_C	T_1	A	X_m	D	α
$^2\mathrm{H}+{}^2\mathrm{H}$	1	23	0.292	1	Equation (8)	0.91	1	23	0.292	1	Equation (9)	0.91
$^2\mathrm{H}+{}^4\mathrm{He}$	1	23	0.292	1	Equation (7)	0.91	1	23	0.292	1	Equation (10)	0.91
$^2\mathrm{H}+{}^9\mathrm{Be}$	1	23	0.292	1	Equation (8)	0.91	1	50	0.292	1	Equation (8)	0.91
$^2\mathrm{H}+{}^{12}\mathrm{C}$	6	23	0.292	1	Equation (8)	0.91	0.8	40	0.5	1	Equation (8)	0.91
$^2\mathrm{H}+{}^{16}\mathrm{O}$	1	23	0.292	1	Equation (8)	0.91	1	55	0.292	1	Equation (8)	0.91
$^2\mathrm{H}+{}^{24}\mathrm{Mg}$	1	23	0.292	1	Equation (8)	0.91	1	100	0.292	1	Equation (8)	0.91
$^2\mathrm{H}+{}^{27}\mathrm{Al}$	1	23	0.292	1	Equation (8)	0.91	1	100	0.292	1	Equation (8)	0.91
$^2\mathrm{H}+{}^{28}\mathrm{Si}$	1	23	0.292	1	Equation (8)	0.91	1	80	0.292	1	Equation (8)	0.91
$^2\mathrm{H}+{}^{40}\mathrm{Ca}$	1	23	0.292	1	Equation (8)	0.91	1	120	0.292	1	Equation (8)	0.91
$^2\mathrm{H}+{}^{48}\mathrm{Ti}$	1	23	0.292	1	Equation (8)	0.91	1	100	0.292	1	Equation (8)	0.91
$^2\mathrm{H}+{}^{51}\mathrm{V}$	1	23	0.292	1	Equation (8)	0.91	0.6	100	0.292	1	Equation (8)	0.91
$^2\mathrm{H}+{}^{56}\mathrm{Fe}$	1	23	0.292	1	Equation (8)	0.91	0.7	200	0.292	1	Equation (8)	0.91
$^2\mathrm{H}+{}^{59}\mathrm{Ni}$	1	23	0.292	1	Equation (8)	0.91	1	110	0.292	1	Equation (8)	0.91
$^2\mathrm{H}+{}^{64}\mathrm{Cu}$	1	23	0.292	1	Equation (8)	0.91	0.6	50	0.292	1	Equation (8)	0.91
$^2\mathrm{H}+{}^{65}\mathrm{Zn}$	1	23	0.292	1	Equation (8)	0.91	0.7	100	0.292	1	Equation (8)	0.91
$^2\mathrm{H}+{}^{89}\mathrm{Y}$	1	23	0.292	1	Equation (8)	0.91	1	240	0.292	1	Equation (8)	0.91
$^2\mathrm{H}+{}^{91}\mathrm{Zr}$	1	23	0.292	1	Equation (8)	0.91	1.1	300	0.292	1	Equation (8)	0.91
$^2\mathrm{H}+{}^{103}\mathrm{Rh}$	1	23	0.292	1	Equation (8)	0.91	0.95	100	0.292	1	Equation (8)	0.91
$^2\mathrm{H}+{}^{108}\mathrm{Ag}$	1	23	0.292	1	Equation (8)	0.91	1	100	0.292	1	Equation (8)	0.91
$^2\mathrm{H}+{}^{136}\mathrm{Xe}$	1	23	0.292	1	Equation (8)	0.91	1	23	0.292	1.18	Equation (8)	0.91
$^2\mathrm{H}+{}^{112,116}\mathrm{Sn}$	1	23	0.292	1	Equation (8)	0.91	1	400	0.292	1	Equation (8)	0.91
$^2\mathrm{H}+{}^{118,120}\mathrm{Sn}$	1	23	0.292	1	Equation (8)	0.91	0.9	600	0.292	1	Equation (8)	0.91
$^2\mathrm{H}+{}^{119}\mathrm{Sn}$	1	23	0.292	1	Equation (8)	0.91	1	40	0.292	1	Equation (8)	0.91
$^2\mathrm{H}+{}^{124}\mathrm{Sn}$	1	23	0.292	1	Equation (8)	0.91	0.9	500	0.292	1	Equation (8)	0.91
$^2\mathrm{H}+{}^{159}\mathrm{Tb}$	1	23	0.292	1	Equation (8)	0.91	1	500	0.292	1	Equation (8)	5
$^2\mathrm{H}+{}^{181}\mathrm{Ta}$	1	23	0.292	1	Equation (8)	0.91	1.25	800	0.292	1	Equation (8)	5
$^2\mathrm{H}+{}^{197}\mathrm{Au}$	1	23	0.292	1	Equation (8)	0.91	1.2	800	0.292	1	Equation (8)	5
$^2\mathrm{H}+{}^{207}\mathrm{Pb}$	1	23	0.292	1	Equation (8)	0.91	1.07	800	0.292	1	Equation (8)	5
$^2\mathrm{H}+{}^{209}\mathrm{Bi}$	1	23	0.292	1	Equation (8)	0.91	1	800	0.292	1	Equation (8)	5

5. Discussion and limitations

It should be noted that not many literature data are available for most systems. Since more than one parameter is changed simultaneously, it could be that a better combination of parameter values exists, but more data would be needed to find the optimal combination. For example, a few different combinations of T_1 and R_c parameters could fit the existing data as well (especially for the cases in which only one data point is available), but with data at other energies, the optimal combination could be identified.

It also should be noted that optimisations are proposed only for the systems for which literature data are available. Nevertheless, the consistency in the optimisations for those systems suggests that the parameters should be adjusted for all systems. For example, it is systematic that T_1 tends to increase as a function of A_T, given a certain projectile.

6. The impact of the optimisation of the Tripathi model on the HK model

The PHITS MC code uses a semi-empirical parametrisation called 'Hybrid-Kurotama' (HK) [80]. It is based on the black sphere ('Kurotama' in Japanese) cross-section formula, extended to low energies by smoothly connecting it to the Tripathi parametrisation. Since the HK model makes use of the Tripathi model at low energies, a systematic study was conducted about the consequences of using the optimised Tripathi model in the HK calculations.

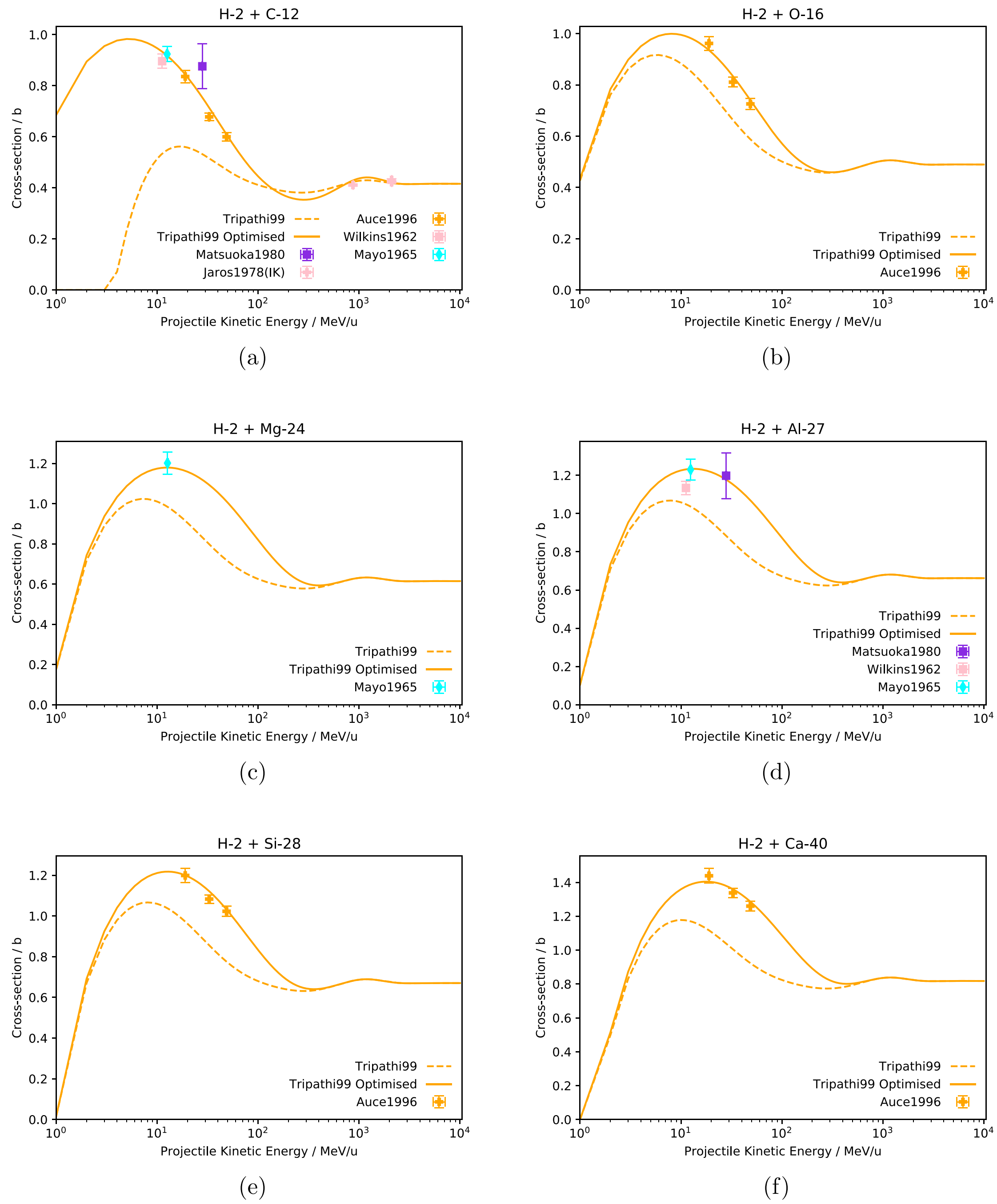

Figure 10. Comparison between the results obtained for ^{2}H using Tripathi99 with the parameters reported in [25] and in this work (see table 4). The experimental data from the database are plotted as well. IK stands for inverse kinematics. Data in panel (a) are from [49, 60–63], in panels (b), (e), and (f) from [61], in panel (c) from [63], and in panel (d) from [60, 62, 63].

Concerning ^{2}H projectiles, the usage of the optimised Tripathi model is either not beneficial or does not make any significant difference in the HK model, with the only exception of Ni targets. A few examples are reported in figure 13 for systems of interest for space and radiation therapy applications. In particular, for the case of ^{2}H + ^{12}C, a curve between the two would fit the existing literature data.

The systems involving ^{3}He projectiles do not show any particular improvement due to the usage of the optimised Tripathi model. Nevertheless, the fit with the HK that uses the original Tripathi model is better in a few cases. Examples are reported in figure 14.

Differently, the HK model fits literature data better when making use of the optimised Tripathi model for all systems involving ^{4}He projectiles, with the exception of extremely heavy targets, i.e. Np and Pu. For a few

Table 5. Recommendations for parameters R_C, T_1, and α to be used for ^{3}He projectiles in Tripathi99 [25]. The parameters from the original model are compared to the parameters recommended in this work. Systems that did not require any change in these parameters (e.g. $^3\mathrm{He} + {}^{12}\mathrm{C}$, ^{27}Al) are not reported.

	Tripathi99 [25]			This work		
	R_C	T_1	α	R_C	T_1	α
$^3\mathrm{He} + {}^{9}\mathrm{Be}$	1	40	0.91	1	50	0.91
$^3\mathrm{He} + {}^{16}\mathrm{O}$	1	40	0.91	1	50	0.91
$^3\mathrm{He} + {}^{28}\mathrm{Si}$	1	40	0.91	1	65	0.91
$^3\mathrm{He} + {}^{40}\mathrm{Ca}$	1	40	0.91	1	55	0.91
$^3\mathrm{He} + {}^{58}\mathrm{Ni}$	1	40	0.91	0.6	60	0.91
$^3\mathrm{He} + {}^{60}\mathrm{Ni}$	1	40	0.91	1	70	0.91
$^3\mathrm{He} + {}^{112}\mathrm{Sn}$	1	40	0.91	1	90	0.91
$^3\mathrm{He} + {}^{116}\mathrm{Sn}$	1	40	0.91	0.5	70	0.91
$^3\mathrm{He} + {}^{118}\mathrm{Sn}$	1	40	0.91	0.5	75	0.91
$^3\mathrm{He} + {}^{120}\mathrm{Sn}$	1	40	0.91	0.7	80	0.91
$^3\mathrm{He} + {}^{207}\mathrm{Pb}$	1	40	0.91	1	50	5

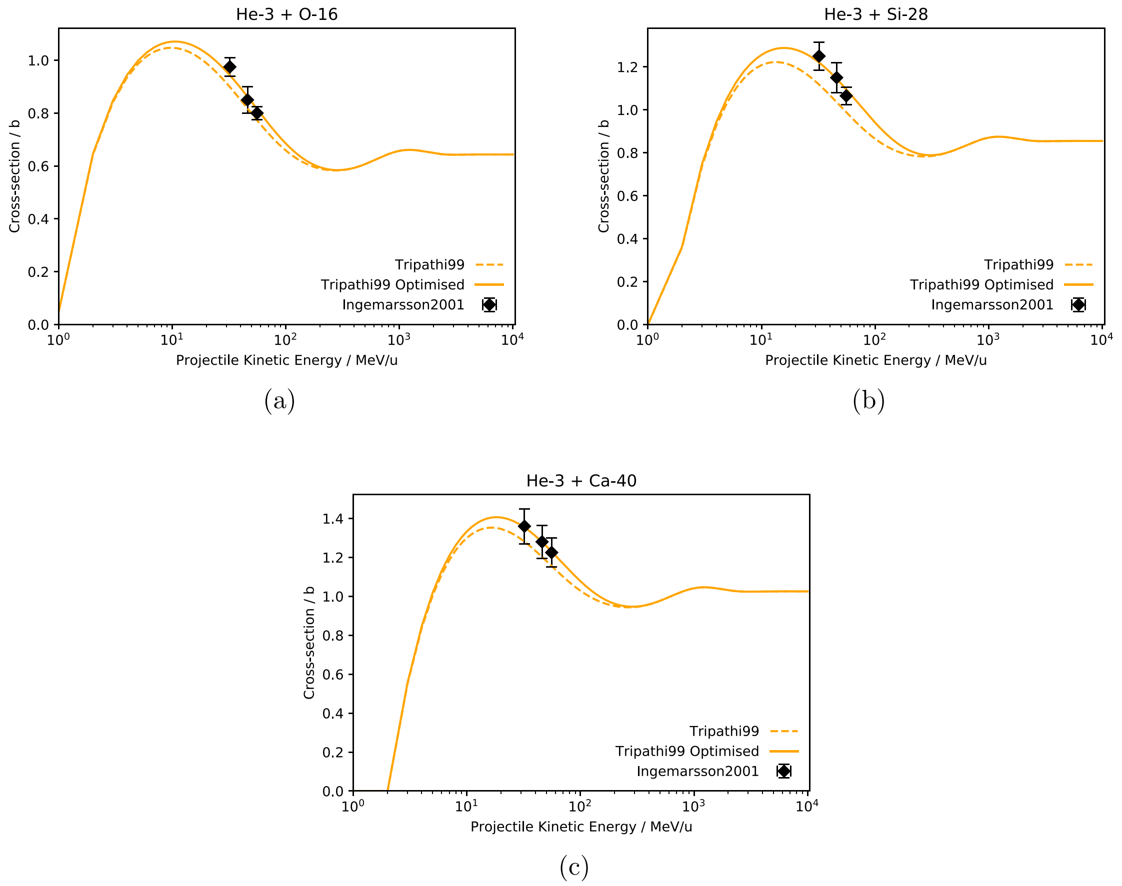

Figure 11. Comparison between the results obtained for ^{3}He using Tripathi99 with the parameters reported in [25] and in this work (see table 5). Data are from [65].

other systems including ^{7}Li, ^{9}Be, ^{9}Be, ^{27}Al, and ^{56}Fe, either the difference is not remarkable or the models fit in a comparable way. A few examples are reported in figure 15. The Labie *et al* [78] dataset suggests for $^4\mathrm{He} + {}^{12}\mathrm{C}$ that the Coulomb barrier should start at higher energies and be steeper. Nevertheless, the unclear trend of the data makes it difficult to trust it enough to start a specific optimisation from it. For the cases of $^4\mathrm{He} + {}^{237}\mathrm{Np}$ and $^4\mathrm{He} + {}^{239}\mathrm{Pu}$, HK making use of the original Tripathi seems to fit the data better. Nevertheless, this can only be stated for the energy range around the Coulomb barrier, which is the only energy range for which experimental data points were measured. In fact, starting from the comparison with

Table 6. Recommendations for parameters to be used for ^{4}He projectiles within Tripathi99, from [25] and this work. Equation (4) comes from [24, 25], equation (11) from [71]. Systems that did not require any change with respect to the parametrisation presented in [25] are not reported. When no specifications about the isotope are there, the recommendations are to be considered valid for every isotope of the element.

	Tripathi99 [25]						This work					
	R_C	T_1	D	D_0	G	A	R_C	T_1	D	D_0	G	A
^{4}He + ^{7}Li	1	40	Equation (4)	2.77	75	0.292	1	40	Equation (4)	2.95	75	0.292
^{4}He + ^{9}Be	1	25	Equation (4)	2.77	300	0.292	7	50	Equation (11)	2.2	50	1.4
^{4}He + ^{12}C	1	40	Equation (4)	2.77	75	0.292	3.5	50	Equation (11)	2.2	50	0.7
^{4}He + ^{16}O	1	40	Equation (4)	2.77	75	0.292	1	50	Equation (11)	2.4	50	0.292
^{4}He + ^{20}Ne	1	40	Equation (4)	2.77	75	0.292	1	40	Equation (4)	3	75	0.292
^{4}He + ^{27}Al	1	25	Equation (4)	2.77	300	0.292	1	20	Equation (4)	2.5	300	0.292
^{4}He + ^{28}Si	1	40	Equation (4)	2.77	75	0.292	1	50	Equation (11)	2.4	50	0.292
^{4}He + ^{40}Ca	1	40	Equation (4)	2.77	75	0.292	1	100	Equation (4)	2.77	75	0.292
^{4}He + ^{48}Ti	1	40	Equation (4)	2.77	75	0.292	1	40	Equation (4)	3	300	0.292
^{4}He + ^{51}V, ^{52}Cr	1	40	Equation (4)	2.77	75	0.292	1.2	40	Equation (4)	3	300	0.292
^{4}He + ^{56}Fe	1	40	Equation (4)	2.77	300	0.292	1.2	40	Equation (4)	3	300	0.292
^{4}He + ^{59}Co	1	40	Equation (4)	2.77	75	0.292	1.1	40	Equation (4)	3	300	0.292
^{4}He + Ni	1	40	Equation (4)	2.77	75	0.292	1.2	80	Equation (4)	3	300	0.292
^{4}He + ^{64}Cu	1	40	Equation (4)	2.77	75	0.292	1.2	80	Equation (4)	3.2	300	0.292
^{4}He + ^{65}Zn	1	40	Equation (4)	2.77	75	0.292	1.1	80	Equation (4)	3.2	300	0.292
^{4}He + ^{91}Zr, ^{93}Nb, ^{96}Mo	1	40	Equation (4)	2.77	75	0.292	1.1	80	Equation (4)	3.4	300	0.292
^{4}He + ^{108}Ag	1	40	Equation (4)	2.77	75	0.292	1	80	Equation (4)	3.4	300	0.292
^{4}He + Sn	1	40	equation (4)	2.77	75	0.292	1.1	80	Equation (4)	3.4	300	0.292
^{4}He + ^{181}Ta	0.6	40	Equation (4)	2.77	75	0.292	1.1	80	Equation (4)	3.4	300	0.292
^{4}He + ^{197}Au	0.6	40	Equation (4)	2.77	75	0.292	1	80	Equation (4)	3.4	300	0.292
^{4}He + ^{207}Pb, ^{209}Bi, ^{232}Th	1	40	Equation (4)	2.77	75	0.292	1.1	75	Equation (4)	3.7	300	0.292
^{4}He + ^{237}Np, ^{239}Pu	1	40	Equation (4)	2.77	75	0.292	1.15	75	Equation (4)	3.7	300	0.292

other heavy-target systems such as ^{4}He + ^{64}Cu and ^{4}He + ^{207}Pb, there is evidence that HK making use of the optimised Tripathi model fits the literature data better at intermediate energy ranges.

The case of ^{4}He + ^{9}Be is particularly interesting (See figure 16). In fact, it is one of the systems that required the most significant changes in the parameters (see table 6). The Ingemarsson2000 dataset [72], in fact, suggested that the Coulomb barrier should start at higher energies and be steeper. Therefore, large changes in R_c were made. HK that makes use of the optimised Tripathi reproduces the trend of the data better, but the fit with the data is lost due to the multiplication factors applied to the Tripathi model in the HK subroutine.

For what concerns systems involving lithium projectiles, in all cases the use of the optimised Tripathi model in the HK subroutine turned out to be beneficial. Figure 17 shows the results for different Li projectiles on Si targets.

For what concerns ^{9}Be projectiles, for all systems for which optimisations are proposed within this work (see table 2), only high-energy data were measured, which does not affect the changes in HK model due to the optimisation since the HK subroutine only makes use of Tripathi at low energies. The only exceptions are ^{12}C and ^{64}Cu targets, which are shown in figure 18. The differences between the two models for the case of ^{9}Be + ^{12}C is minimal. Nevertheless, the HK that makes use of the original Tripathi model fits better. For the case of ^{9}Be + ^{64}Cu, the HK making use of the optimised Tripathi model fits better because the proposed parameter changes are particularly significant for this systems (see table 2) with the aim of fitting the lower-energy point of the Saint Laurent1989 dataset [42], at least within the error bars (see figure 3).

The outcome for ^{12}C projectiles is that in an equal number of cases HK that uses the original and optimised Tripathi fits better. One example per case are reported in figure 19. To be noticed that Shapira1982 [52] are among the rare cases of very-low-energy data points and the HK model making use of the optimised Tripathi model fits them better. This brings more evidence that the HK subroutine benefits from the Tripathi optimisation in the Coulomb-barrier energy region.

For the case of ^{16}O projectiles, HK that uses the optimised Tripathi fits the single data point better, while for what concerns ^{20}Ne projectiles, the two models fit the data as well.

Concerning radioactive ions (see table 3), there are only experimental data points at energies where the two models are identical, i.e. in the high-energy range where the usage of different Tripathi parametrisations does not affect the HK model.

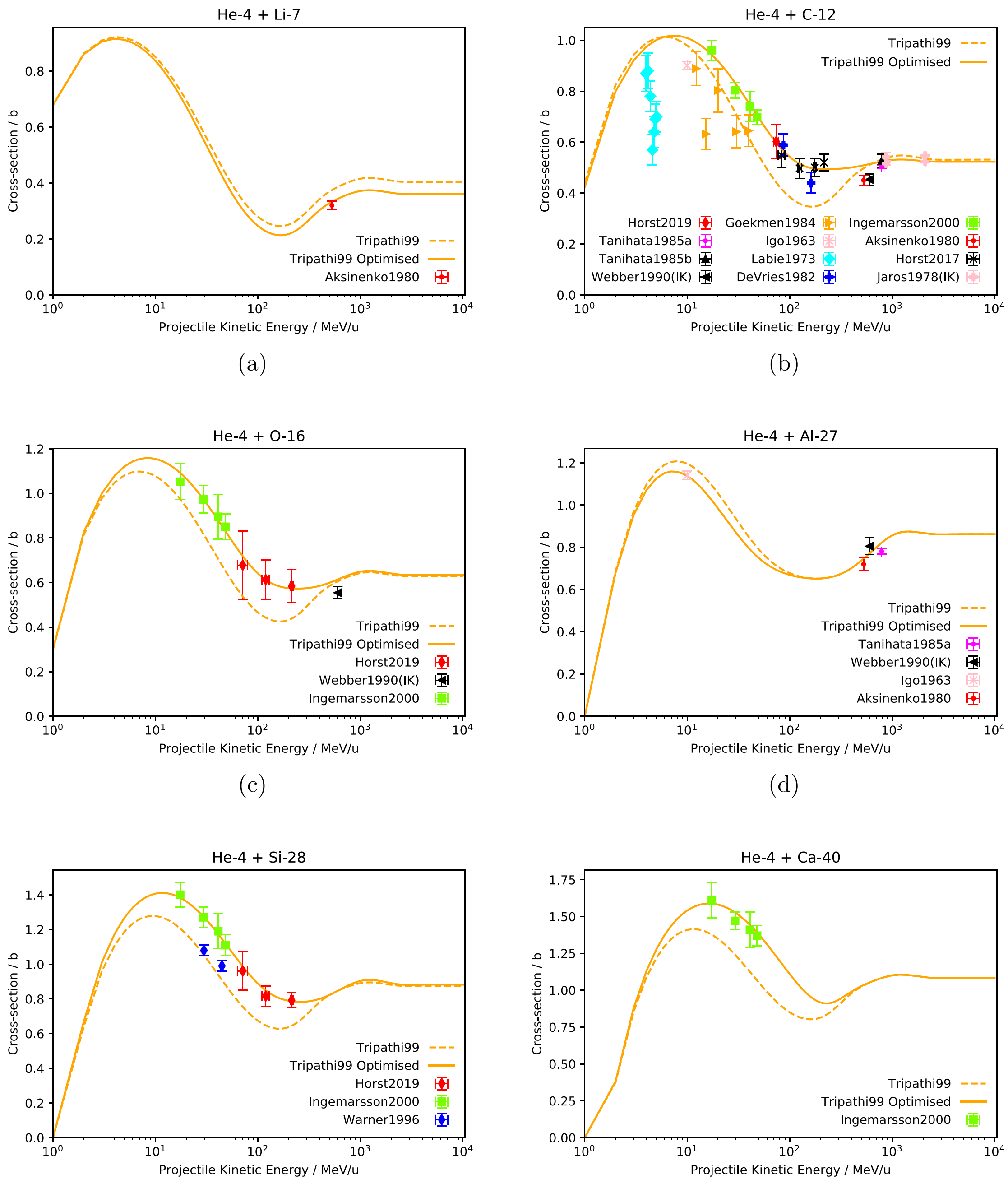

Figure 12. Comparison between the results obtained for ^{4}He using Tripathi99 with the parameters reported in [25] and in this work (see table 6). The experimental data from the database are plotted as well. IK stands for inverse kinematics. Data in panel (a) are from [45], in panel (b) from [43, 45, 49, 71–79], in panel (c) from [43, 71, 72], in panel (d) from [43, 45, 74, 77], in panel (e) from [32, 71, 72], and in panel (f) from [72].

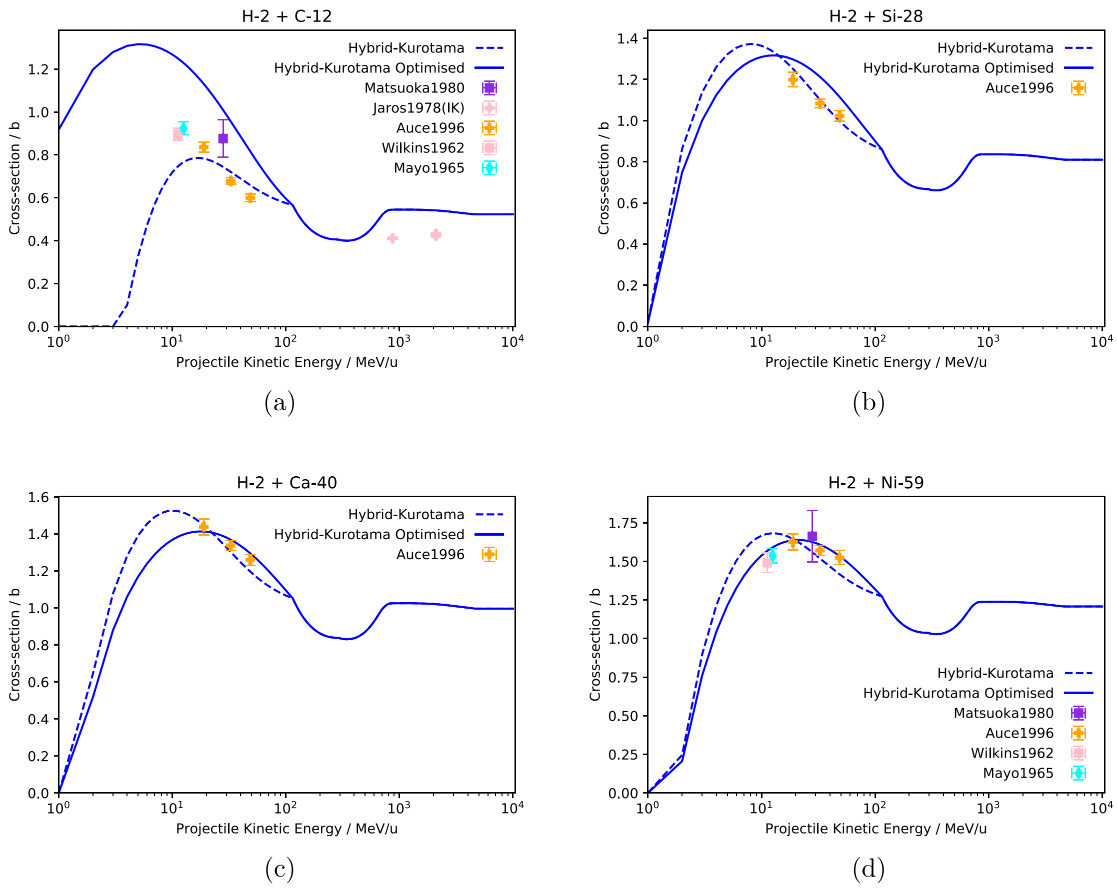

Figure 13. Comparison between the results obtained for ^{2}H projectiles with the HK subroutine making use of the optimised (see table 4) and unoptimised Tripathi model, respectively 'Hybrid-Kurotama Opt' and 'Hybrid-Kurotama'. IK stands for inverse kinematics. Data in panel (a) are from [49, 60–63], in panels (b) and (c) from [61], and in panel (d) from [60–63].

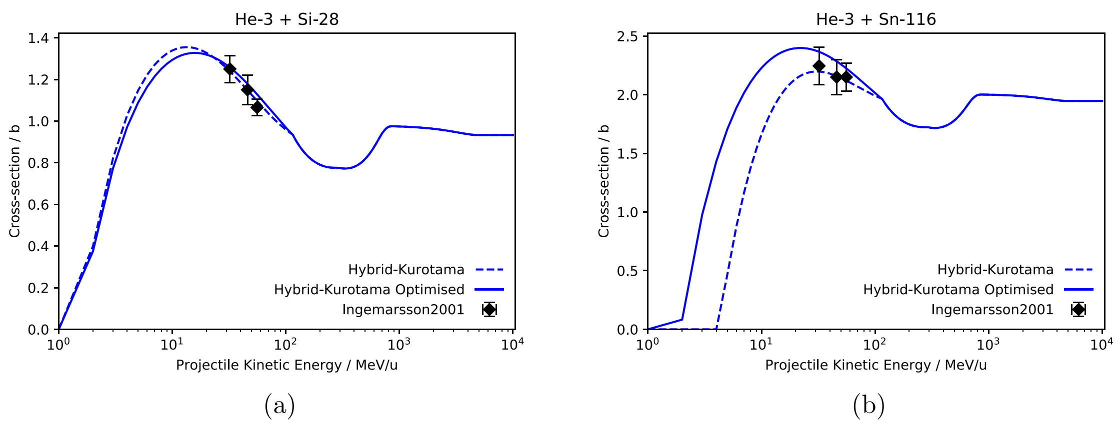

Figure 14. Comparison between the results obtained for ^{3}He projectiles with the HK subroutine making use of the optimised (see table 5) and unoptimised Tripathi model, respectively 'Hybrid-Kurotama Opt' and 'Hybrid-Kurotama'. Data are from [72].

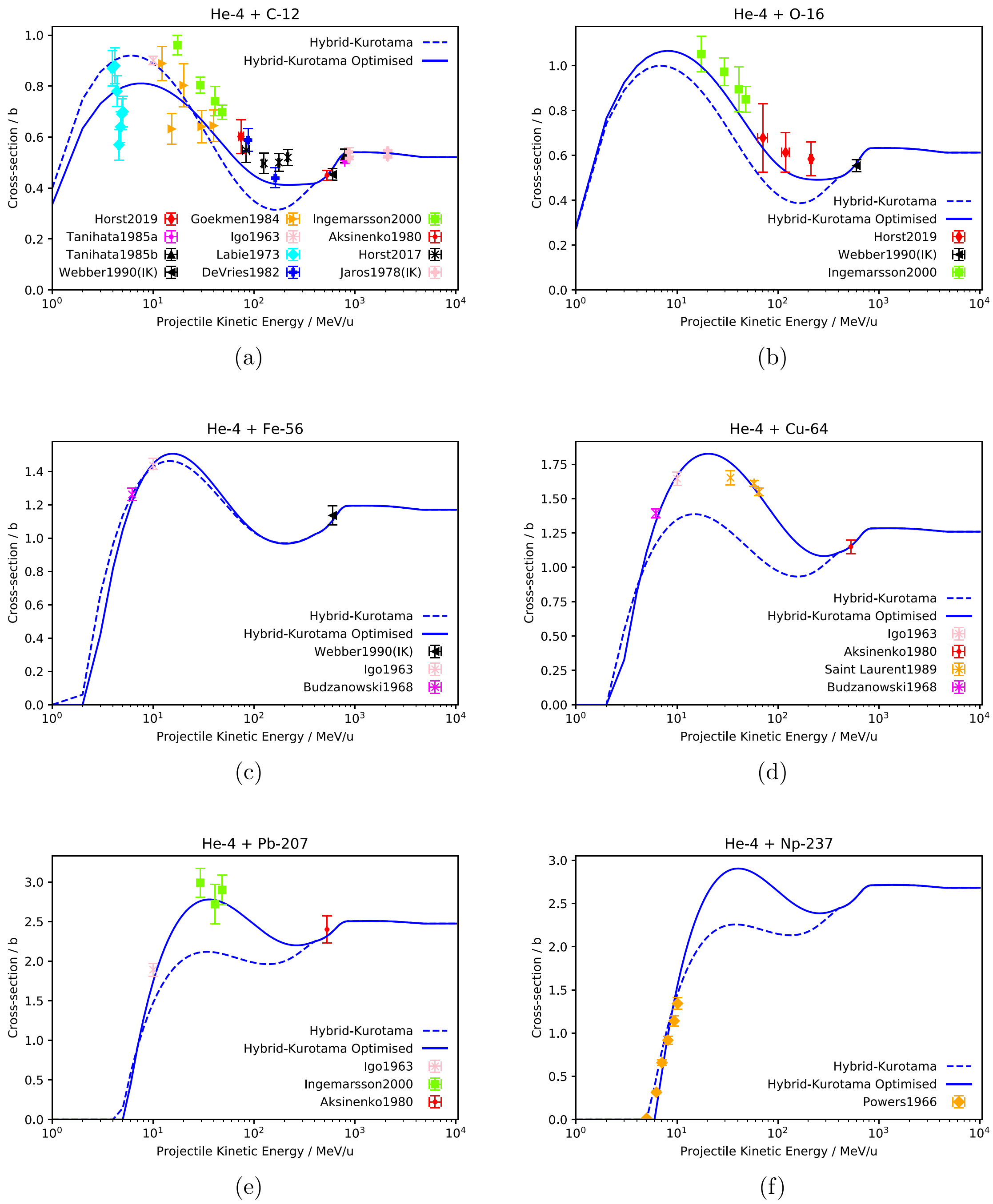

Figure 15. Comparison between the results obtained for ^{4}He projectiles with the HK subroutine making use of the optimised (see table 6) and unoptimised Tripathi model, respectively 'Hybrid-Kurotama Opt' and 'Hybrid-Kurotama'. IK stands for inverse kinematics. Data in panel (a) are from [43, 45, 49, 71–79], in panel (b) from [43, 71, 72], in panel (c) from [43, 77, 81], and in panel (d) from [42, 45, 77, 81], in panel (e) from [45, 72, 77], in panel (f) from [82].

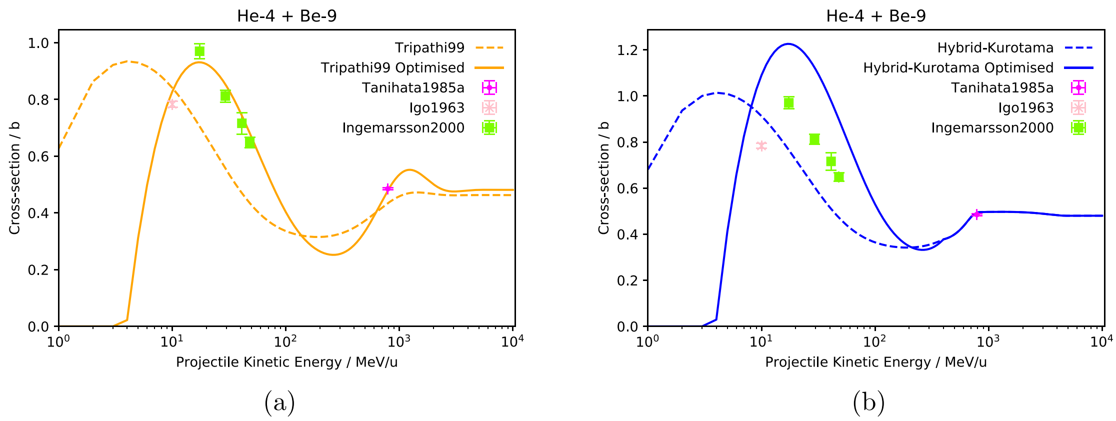

Figure 16. Comparison between the results obtained for ^{4}He + ^{9}Be with the HK subroutine making use of the optimised (see table 6) and unoptimised Tripathi model, respectively 'Hybrid-Kurotama Opt' and 'Hybrid-Kurotama'. Data are from [72, 74, 77].

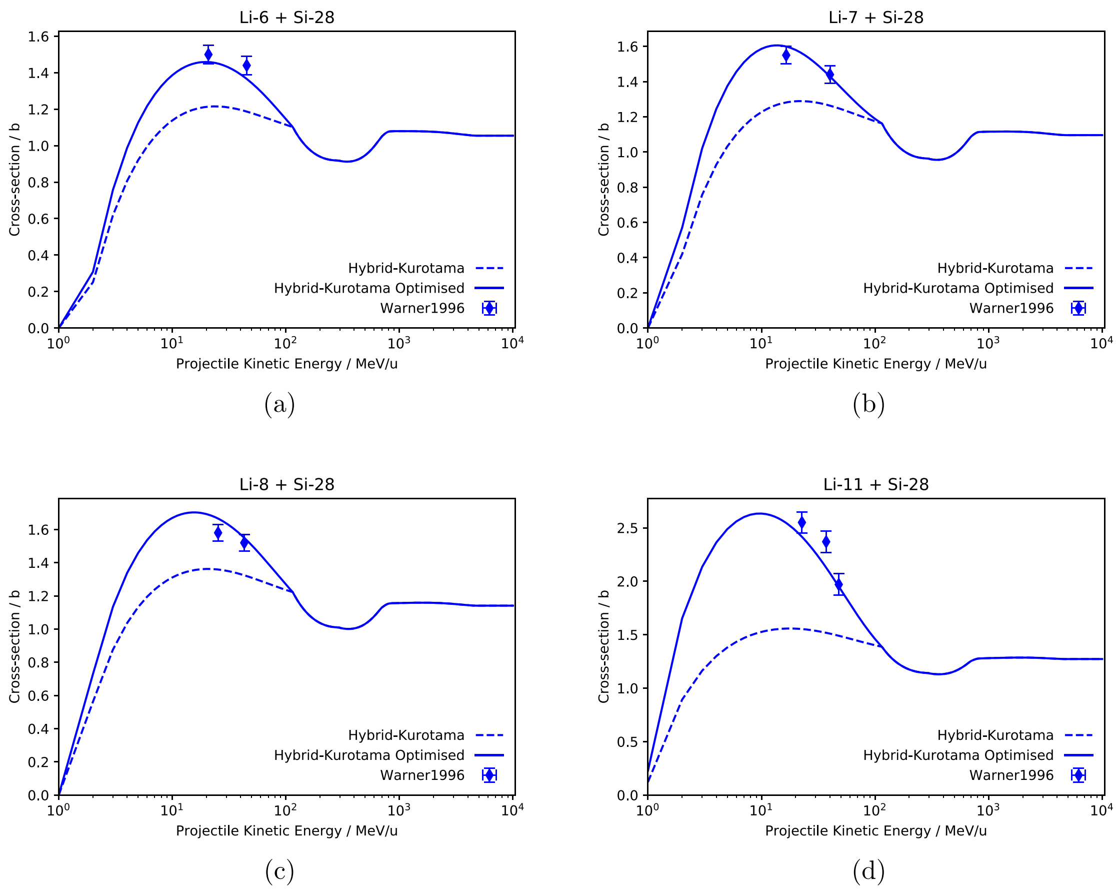

Figure 17. Comparison between the results obtained for different Li isotopes with the HK subroutine making use of the optimised (see table 1) and unoptimised Tripathi model, respectively 'Hybrid-Kurotama Opt' and 'Hybrid-Kurotama'. Data are from [32].

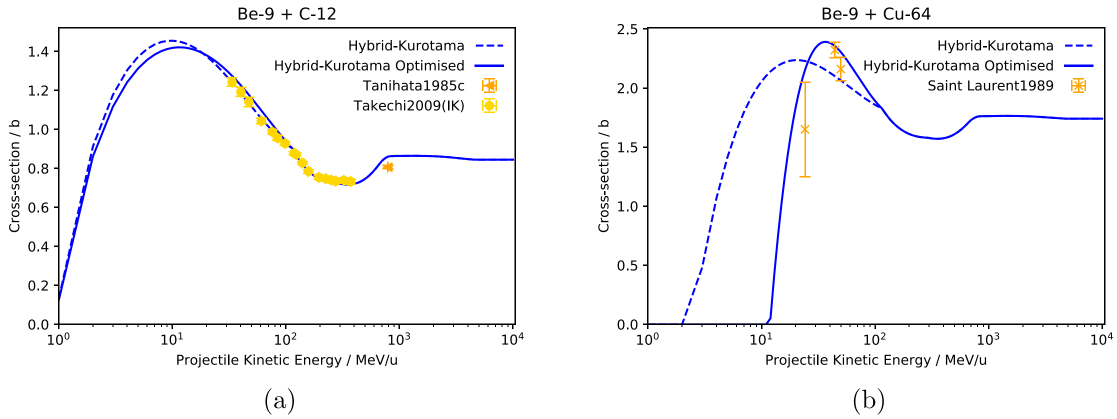

Figure 18. Comparison between the results obtained for ^{9}Be projectiles with the HK subroutine making use of the optimised (see table 2) and unoptimised Tripathi model, respectively 'Hybrid-Kurotama Opt' and 'Hybrid-Kurotama'. IK stands for inverse kinematics. Data in panel (a) are from [31, 41] and in panel (b) [42].

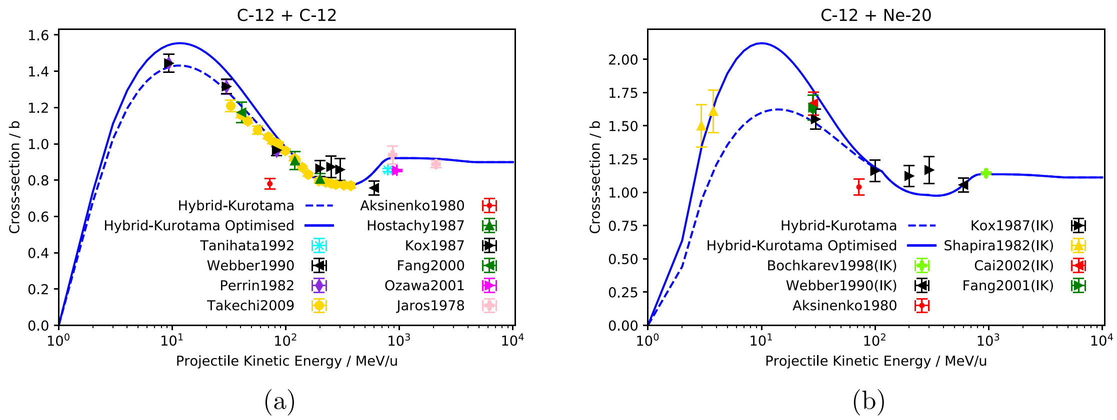

Figure 19. Comparison between the results obtained for ^{12}C projectiles with the HK subroutine making use of the optimised (see table 2) and unoptimised Tripathi model, respectively 'Hybrid-Kurotama Opt' and 'Hybrid-Kurotama'. IK stands for inverse kinematics. Data in panel (a) are from [35, 40, 41, 43–49] and in panel (b) [40, 43, 45, 50–53].

7. Conclusions

In this work, literature data from the open-access GSI-ESA-NASA cross-section database [7, 8] were used to propose an optimised version of the Tripathi model [24, 25]. The use of the optimised model could potentially improve the results of MC and deterministic radiation transport codes used for radiation protection in space, radiation therapy applications, or other technical fields where e.g. deuteron interactions are relevant. The optimised Tripathi parametrisation presented in this work fits the data best for all systems for which experimental reaction cross-section data have been measured. Nevertheless, these optimisations should be tested by comparing the outcome of MC simulations against experimental results of e.g. absorbed dose curves, as it was done for the Horst D factor corrections [5, 70], or other available datasets such as particle spectra behind materials. It is to be noted that, even if optimisations are proposed only for the systems for which literature data are available, their consistency suggests that the parameters should be adjusted for all systems accordingly.

Additionally, a systematic study was conducted with the aim of understanding if the HK subroutine used in the PHITS MC code benefits from the proposed Tripathi model optimisations. Considerations can be made only for systems for which low and intermediate-energy range data were measured because only these ranges are affected by the change in the Tripathi model used in HK. The outcome is that it is recommended to make use of the optimised Tripathi model for ^{4}He and Li projectiles impinging on any of the targets included in the optimisation, and for ^{9}Be, ^{16}O, and ^{20}Ne projectiles on ^{64}Cu targets. For the other systems for which optimisations to the Tripathi model are proposed within this work, it is recommended to continue using the original Tripathi parameters within HK or to use other specific parameter optimisations. For the case of ^{12}C projectile, considerations must be done system by system. In general, HK benefits from the Tripathi optimisations in the Coulomb-barrier energy range (except for the very first few MeV/u of it).

Data availability statement

The nuclear cross-section database is available at: www.gsi.de/fragmentation.

Acknowledgments

The work was supported in the framework of the work package 200 of the ROSSINI3 Project (ESA Contract No. 4000125785/18/NL/GLC), which was a 2 year Project started in December 2018, funded by ESA ESTEC and led by Thales Alenia Space Italia.

ORCID iDs

F Luoni https://orcid.org/0000-0002-9808-4251
F Horst https://orcid.org/0000-0003-0707-0856
M Durante https://orcid.org/0000-0002-4615-553X

References

[1] Townsend L W, Cucinotta F A and Heilbronn L H 2002 Nuclear model calculations and their role in space radiation research *Adv. Space Res.* **30** 907–16
[2] Norbury J W, Miller J, Adamczyk A M, Heilbronn L H, Townsend L W, Blattnig S R, Norman R B, Guetersloh S B and Zeitlin C J 2012 Nuclear data for space radiation *Radiat. Meas.* **47** 315–63
[3] Durante M and Cucinotta F A 2011 Physical basis of radiation protection in space travel *Rev. Mod. Phys.* **83** 1245–81
[4] Chancellor J C, Scott G B I and Sutton J P 2014 Space radiation: the number one risk to astronaut health beyond low earth orbit *Life* **4** 491–510
[5] Aricò G, Ferrari A, Horst F, Mairani A, Reidel C A, Schuy C and Weber U 2019 Developments of the nuclear reaction and fragmentation models in FLUKA for ion collisions at therapeutic energies *CERN Proc.* **1** 321–6
[6] Lühr A, Hansen D C, Teiwes R, Sobolevsky N, Jäkel O and Bassler N 2012 The impact of modeling nuclear fragmentation on delivered dose and radiobiology in ion therapy *Phys. Med. Biol.* **57** 5169
[7] Luoni F *et al* 2021 Total nuclear reaction cross-section database for radiation protection in space and heavy-ion therapy applications *New J. Phys.* **23** 101201
[8] (Available at: www.gsi.de/fragmentation)
[9] (Available at: http://geant4.cern.ch/)
[10] Agostinelli S *et al* 2003 Geant4-a simulation toolkit *Nucl. Instrum. Methods Phys. Res.* A **506** 250–303
[11] Allison J *et al* 2006 Geant4 developments and applications *IEEE Trans. Nucl. Sci.* **53** 270–8
[12] Allison J *et al* 2016 Recent developments in Geant4 *Nucl. Instrum. Methods Phys. Res.* A **835** 186–225
[13] Iwase H, Niita K and Nakamura T 2002 Development of general-purpose particle and heavy ion transport Monte Carlo code *J. Nucl. Sci. Technol.* **39** 1142–51
[14] PHITS user's manual Version 3.31 (available at: https://phits.jaea.go.jp/manual/manualE-phits.pdf)
[15] Böhlen T T, Cerutti F, Chin M P W, Fassò A, Ferrari A, Ortega P G, Mairani A, Sala P R, Smirnov G, Vlachoudis V 2014 The FLUKA Code: Developments and Challenges for High Energy and Medical Applications *Nucl. Data Sheets* **120** 211–4
[16] Andersen V *et al* 2004 The FLUKA code for space applications: recent developments *Adv. Space Res.* **34** 1302–10 Space Life Sciences: Radiation Risk Assessment and Radiation Measurements in Low Earth Orbit
[17] Wilson J W, Badavi F F, Cucinotta F A, Shinn J L, Badhwar G D, Silberberg R, Tsao C H, Townsend L W and Tripathi R L 1995 Hzetrn: description of a free-space ion and nucleon transport and shielding computer program *Technical Report* 3495 NASA
[18] Krämer M, Jäkel O, Haberer T, Kraft G, Schardt D and Weber U 2000 Treatment planning for heavy-ion radiotherapy: physical beam model and dose optimization *Phys. Med. Biol.* **45** 3299–317
[19] Kraemer M, Scifoni E, Giraudo M and Durante M 2018 Towards a space-trip: a space radiation version of the trip98 code *Technical Report* GSI-FAIR Scientific Report 2017 p 289
[20] Franco V 1987 Quark model for nucleus-nucleus collisions *Phys. Rev.* C **35** 1328–33
[21] Cucinotta F A, Yan C and Saganti P B 2018 2nd-order optical model of the isotopic dependence of heavy ion absorption cross sections for radiation transport studies *Nucl. Instrum. Methods Phys. Res.* B **414** 11–17
[22] Dubey R R, Khandelwal G S, Cucinotta F A and Wilson J W 1996 Microscopic optical model calculations of - nucleus absorption cross sections *J. Phys. G: Nucl. Part. Phys.* **22** 387
[23] Wallace S J 1987 Relativistic equation for nucleon-nucleus scattering *Ann. Rev. Nucl. Part. Sci.* **37** 267–92
[24] Tripathi R K, Cucinotta F A and Wilson J W 1996 Accurate universal parameterization of absorption cross sections *Nucl. Instrum. Methods Phys. Res.* B **117** 347–9
[25] Tripathi R K, Cucinotta F A and Wilson J W 1999 Accurate universal parameterization of absorption cross sections III - light systems *Nucl. Instrum. Methods Phys. Res.* B **155** 349–56
[26] Giraudo M *et al* 2018 Accelerator-based tests of shielding effectiveness of different materials and multilayers using high-energy light and heavy ions *Radiat. Res.* **190** 526–37
[27] Schuy C *et al* 2018 Experimental assessment of lithium hydride's space radiation shielding performance and Monte Carlo benchmarking *Radiat. Res.* **191** 154–61
[28] Naito M *et al* 2020 Investigation of shielding material properties for effective space radiation protection *Life Sci. Space Res.* **26** 69–76
[29] Luoni F *et al* 2022 Dose attenuation in innovative shielding materials for radiation protection in space: measurements and simulations *Radiat. Res.* **198** 107–19

[30] Cronin J W 1999 *Cosmic Rays: The Most Energetic Particles in the Universe* (Springer) pp 278–90
[31] Tanihata I, Hamagaki H, Hashimoto O, Shida Y, Yoshikawa N, Sugimoto K, Yamakawa O, Kobayashi T and Takahashi N 1985 Measurements of interaction cross sections and nuclear radii in the light *p*-shell region *Phys. Rev. Lett.* **55** 2676–9
[32] Warner R E *et al* 1996 Total reaction and 2n-removal cross sections of 20–60 A MeV ^{4,6,8}He, $^{6-9,11}$Li and ^{10}Be on Si *Phys. Rev.* C **54** 1700–9
[33] Westfall G D, Wilson L W, Lindstrom P J, Crawford H J, Greiner D E and Heckman H H 1979 Fragmentation of relativistic ^{56}Fe *Phys. Rev.* C **19** 1309–23
[34] Fukuda M *et al* 1999 Density distribution of ^{8}B studied via reaction cross sections *Nucl. Phys.* A **656** 209–28
[35] Tanihata I *et al* 1992 Determination of the density distribution and the correlation of halo neutrons in ^{11}Li *Phys. Lett.* B **287** 307–11
[36] Kobayashi T 1992 Projectile fragmentation of exotic nuclear beams *Nucl. Phys.* A **538** 343–52
[37] Schardt D, Elsaesser T and Schulz-Ertner D 2010 Heavy-ion tumor therapy: physical and radiobiological benefits *Rev. Mod. Phys.* **82** 383–425
[38] (Available at: www.ptcog.ch/index.php/facilities-in-operation-restricted)
[39] Sokol O *et al* 2017 Oxygen beams for therapy: advanced biological treatment planning and experimental verification *Phys. Med. Biol.* **62** 7798–813
[40] Kox S *et al* 1987 Trends of total reaction cross sections for heavy ion collisions in the intermediate energy range *Phys. Rev.* C **35** 1678–91
[41] Takechi M *et al* 2009 Reaction cross sections at intermediate energies and Fermi-motion effect *Phys. Rev.* C **79** 061601
[42] Saint-Laurent M G *et al* 1989 Total cross sections of reactions induced by neutron-rich light nuclei *Z. Phys.* **332** 457–65
[43] Webber W R, Kish J C and Schrier D A 1990 Total charge and mass changing cross sections of relativistic nuclei in hydrogen, helium and carbon targets *Phys. Rev.* C **41** 520–32
[44] Perrin C *et al* 1982 Direct measurement of the ^{12}C + ^{12}C reaction cross section between 10 and 83 MeV/Nucleon *Phys. Rev. Lett.* **49** 1905–9
[45] Aksinenko V D *et al* 1980 Streamer chamber study of the cross sections and multiplicities in nucleus-nucleus interactions at the incident momentum of 4.5 GeV/c per nucleon *Nucl. Phys.* A **348** 518–34
[46] Hostachy J Y *et al* 1987 Elastic scattering of ^{12}C on ^{12}C at E/A = 120 MeV/u and 200 MeV/u *Phys. Lett.* B **184** 139–43
[47] Fang D Q *et al* 2000 Measurements of total reaction cross sections for some light nuclei at intermediate energies *Phys. Rev.* C **61** 064311
[48] Ozawa A *et al* 2001 Measurements of interaction cross sections for light neutron-rich nuclei at relativistic energies and determination of effective matter radii *Nucl. Phys.* A **691** 599–617
[49] Jaros J *et al* 1978 Nucleus-nucleus total cross sections for light nuclei at 1.55 and 2.89 GeV/c per nucleon *Phys. Rev.* C **18** 2273–92
[50] Fang D Q *et al* 2001 Evidence for a proton halo in ^{27}P through measurements of reaction cross-sections at intermediate energies *Eur. Phys. J.* A **12** 335–9
[51] Bochkarev O V *et al* 1998 Evidence for a neutron skin in ^{20}N *Eur. Phys. J.* A **1** 15–17
[52] Shapira D, Ford J L C and del Campo J G 1982 Reactions of ^{20}Ne with ^{12}C *Phys. Rev.* C **26** 2470–86
[53] Cai X Z *et al* 2002 Existence of a proton halo in ^{23}Al and its significance *Phys. Rev.* C **65** 024610
[54] Llacer J, Chatterjee A, Alpen E L, Saunders W, Andreae S and Jackson H C 1984 Imaging by injection of accelerated radioactive particle beams *IEEE Trans. Med. Imaging* **3** 80–90
[55] Iseki Y, Kanai T, Kanazawa M, Kitagawa A, Mizuno H, Tomitani T, Suda M and Urakabe E 2004 Range verification system using positron emitting beams for heavy-ion radiotherapy *Phys. Med. Biol.* **49** 3179
[56] Durante M and Parodi K 2020 Radioactive beams in particle therapy: past, present and future *Front. Phys.* **8**
[57] Boscolo D *et al* 2021 Radioactive beams for image-guided particle therapy: the barb experiment at GSI *Front. Oncol.* **11** 737050
[58] Ozawa A, Tanihata I, Kobayashi T, Sugahara Y, Yamakawa O, Omata K, Sugimoto K, Olson D, Christie W and Wieman H 1996 Interaction cross sections and radii of light nuclei *Nucl. Phys.* A **608** 63–76
[59] Ozawa A *et al* 1995 Interaction cross-sections and radii of ^{11}C and ^{12}N and effective deformation parameters in light mirror nuclei *Nucl. Phys.* A **583** 807–10
[60] Matsuoka N, Kondo M, Shimizu A, Saito T, Nagamachi S, Sakaguchi H, Goto A and Ohtani F 1980 Deuteron break-up in the fields of nuclei at 56 MeV *Nucl. Phys.* A **345** 1–12
[61] Auce A, Carlson R F, Cox A J, Ingemarsson A, Johansson R, Renberg P U, Sundberg O and Tibell G 1996 Reaction cross sections for 38, 65 and 97 mev deuterons on targets from ^{9}Be to ^{208}Pb *Phys. Rev.* C **53** 2919–25
[62] Wilkins B and Igo G 1962 Total reaction cross sections for 22.4 ev deuterons *Technical Report* LBNL
[63] Mayo S, Schimmerling W, Sametband M J and Eisberg R M 1965 Reaction cross sections for 26.5 meV deuterons *Nucl. Phys.* **62** 393–400
[64] Horst F, Schardt D, Iwase H, Schuy C, Durante M and Weber U 2021 Physical characterization of ^{3}He ion beams for radiotherapy and comparison with ^{4}He *Phys. Med. Biol.* **66** 095009
[65] Ingemarsson A *et al* 2001 Reaction cross sections of intermediate energy 3He-particles on targets from ^{9}Be to ^{208}Pb *Nucl. Phys.* A **696** 3–30
[66] Norbury J W *et al* 2020 Are further cross section measurements necessary for space radiation protection or ion therapy applications? Helium projectiles *Front. Phys.* **8** 409
[67] Grün R, Friedrich T, Krämer M, Zink K, Durante M, Engenhart-Cabillic R and Scholz M 2015 Assessment of potential advantages of relevant ions for particle therapy: a model based study *Med. Phys.* **42** 1037–47
[68] Krämer M *et al* 2016 Helium ions for radiotherapy? Physical and biological verifications of a novel treatment modality *Med. Phys.* **43** 1995–2004
[69] Mairani A *et al* 2022 Roadmap: helium ion therapy *Phys. Med. Biol.* **67** 15TR02
[70] Horst F 2020 Measurement of nuclear reaction cross sections for applications in radiotherapy with protons, helium and carbon ions *PhD Thesis* Justus Liebig University Gießen
[71] Horst F *et al* 2019 Measurement of ^{4}He charge- and mass-changing cross sections on H, C, O and Si targets in the energy range 70–220 MeV/u for radiation transport calculations in ion-beam therapy *Phys. Rev.* C **99** 014603
[72] Ingemarsson A *et al* 2000 New results for reaction cross sections of intermediate energy α-particles on targets from ^{9}Be to ^{208}Pb *Nucl. Phys.* A **676** 3–31
[73] Horst F, Schuy C, Weber U, Brinkmann K T and Zink K 2017 Measurement of charge- and mass-changing cross sections for ^{4}He+^{12}C collisions in the energy range 80-220 MeV/u for applications in ion beam therapy *Phys. Rev.* C **96** 024624
[74] Tanihata I *et al* 1985 Measurements of interaction cross sections and radii of He isotopes *Phys. Lett.* B **160** 380–4

[75] Tanihata I 1985 Nuclear physics using unstable nuclear beams *Hyperfine Interact.* **21** 251–64

[76] Gökmen A, Breuer H, Mignerey A C, Glagola B G, Kwiatkowski K and Viola V E 1984 Fragment mass, energy and angular distributions for the ^{12}C(^{4}He, heavy ion) reaction between 49 and 159 MeV *Phys. Rev.* C **29** 1595–605

[77] Igo G and Wilkins B D 1963 Alpha-particle reaction cross sections at 40 MeV *Phys. Rev.* **131** 1251–3

[78] Labie E, Lega J, Leleux P and Macq P C 1973 Total reaction cross section of α-particles on carbon between 15.8 and 20.1 MeV *Nucl. Phys.* A **205** 81–89

[79] De Vries R M, DiGiacomo N J, Kapustinsky J S, Peng J C, Sondheim W E, Sunier J W, Cramer J G, Loveman R E, Gruhn C R and Wieman H H 1982 Dominance of nucleon-nucleon interactions in $\alpha+^{12}$C total reaction cross sections *Phys. Rev.* C **26** 301–3

[80] Sihver L, Kohama A, Iida K, Oyamatsu K, Hashimoto S, Iwase H and Niita K 2014 Current status of the 'Hybrid Kurotama model' for total reaction cross sections *Nucl. Instrum. Methods Phys. Res.* B **334** 34–39

[81] Budzanowski A, Grotowski K, Kuźmiński J, Niewodniczański H, Strzałkowski A, Sykutowski S, Szmider J and Wolski R 1967 Total reaction cross section and elastic scattering of 24.7 MeV alpha particles in the region of A = 60 nuclei *Nucl. Phys.* A **106** 21–34

[82] Powers J A, Wogman N A and Cobble J W 1966 Mass Distribution in the Fission of Np^{237} and Pu^{239} by intermediate-energy helium ions *Phys. Rev.* **152** 1096–102